This article has been accepted for publication in a future issue of this journal, but has not been fully edited. Content may change prior to final publication. Citation information: DOI 10.1109/JESTPE.2019.2891317, IEEE Journal of Emerging and Selected Topics in Power Electronics

High-Frequency Three-Phase Interleaved LLC Resonant Converter with GaN Devices and Integrated Planar Magnetics

Chao Fei, *Member, IEEE,* Rimon Gadelrab, *Student Member, IEEE,* Qiang Li, *Member, IEEE,* Fred C. Lee, *Life Fellow, IEEE*

Center for Power Electronics Systems
Virginia Tech, Blacksburg, VA 24061 USA

***Abstract*— The LLC converter is deemed the most widely used topology as DC/DC converter in server and telecom applications. To increase the output power and reduce the input and output current ripples, three-phase interleaved LLC converter is becoming more and more popular. It has been demonstrated that three interleaved LLC converter can achieve further efficiency improvement at the 3kW power level. However, the magnetic components for multiphase LLC converter are complex, bulky, and difficult to manufacture in a cost-effective manner. In this paper, a high-frequency GaN based three-phase LLC converter is employed to address these aforementioned challenges. With GaN operating at 1MHz, all magnetics components, namely, 3 inductors and 3 transformers, can be integrated in one common structure while all magnetic windings implemented in a compact 4-layer PCB with 3oz copper. The proposed structure can be easily manufactured cost-effectively in high quality. Furthermore, shielding techniques for full-bridge secondary has been investigated, and additional 2-layer shielding has been integrated to reduce common-mode (CM) noise. A 1MHz 3kW 400V/48V three-phase LLC converter is demonstrated, and peak efficiency of 97.7% and power density of 600W/inch^3 (37kW/L) are achieved.**

***Keywords*— LLC resonant converter, interleaving, magnetic integration, high-frequency transformer, gallium nitride (GaN).**

I. Introduction

The LLC converter is the most widely used topology as DC/DC converter for front-end power supplies in server and telecom applications. The LLC resonant converters have the benefit of zero-voltage-switching (ZVS) for all the load conditions, can maintain a low turn-off current for primary switches and zero-current-switching (ZCS) for the synchronous rectifiers (SRs), thus LLC converter can achieve both high efficiency and high power density [1]-[6]. Since LLC converter has small turn-off current, the *dv/dt* at the primary switching node is also small, which helps reduce electromagnetic interference [5]. In comparison with soft-switching PWM converters, LLC converters can achieve a higher switching frequency f_S with better efficiency, resulting in a higher power density and lower total cost [2][4].

With the fast development of information technology (IT), the total power consumption of today's data centers is becoming noticeable. In 2014, data centers in the U.S. consumed an estimated 70 billion kWh, representing about 1.8% of total U.S. electricity consumption [7]. Moreover, as cloud computing and big data are continuing to growing rapidly, data centers is expected to consume more and more energy. The current practice of data center power architecture is illustrated in Fig. 1(a), where all major processor/memory devices are powered from a 12V bus. Such structure has limited total system efficiency due to many energy conversion stages and large copper loss at 12V bus, and high cost for connectors and bus bar at 12V bus. To mitigate the heavy bus-bar loss and reduce energy conversion stages in the power distribution path, Google is promoting a new data center design with 48V distribution bus instead of 12V bus [8]-[13]. Power architecture with 48V bus, shown in Fig. 1(b), has the benefits of less distribution losses at 48V bus compared to 12V bus, compatibility with 48V telecom power supply ecosystem, cost-effective in-rack uninterruptible power source (UPS), and safe bus bar voltage for human body.

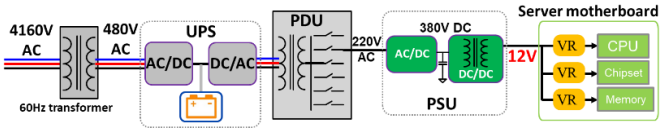

(a)

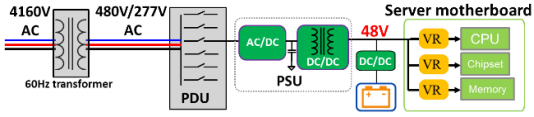

(b)

Fig. 1 Comparison of data center power architectures. (a) Current architecture with 12V bus. (b) Alternative architecture with 48V bus.

In datacenter architecture with 12V bus, most AC/12V PSU are designed for 1kW output power [14]. As power demand for datacenter architecture keeps increasing, the AC/48V PSU is normally designed for 3kW output power. To increase the output power, paper [15] changes primary side from half-bridge structure to full-bridge structure, but output current ripples also increase as output power increases. To increase output power

This work was supported by the Power Management Consortium in the Center for Power Electronics Systems (CPES), Virginia Tech.

This article has been accepted for publication in a future issue of this journal, but has not been fully edited. Content may change prior to final publication. Citation information: DOI 10.1109/JESTPE.2019.2891317, IEEE Journal of Emerging and Selected Topics in Power Electronics

while maintaining a small output current ripples, two-phase interleaved LLC converters have been proposed in [16]-[20], but additional switches, components, and control algorithm are required in order to achieve current sharing. Three-phase interleaved LLC converter can achieve automatic current sharing by interconnecting the three phases in certain ways, including connecting the primary sides to a common Y-node (Y-Primary) [21], connecting the secondary sides to a common Y-node (Y-Secondary) [22], employing a delta-connect resonant capacitor network for primary sides (primary Δ-Cr network) [23], and other variations [24]. Furthermore, the primary and secondary RMS current can be reduced due to interaction between three phases [21]-[23], and three inductors and three transformers can be integrated into one magnetic component [23]. Other three-phase interleaved LLC converters are presented in [25][26], but they both requires additional balancing transformer. To sum up, three-phase interleaved LLC converter is considered as a superior candidate for 3kW 400V/48V DC/DC converter with the benefits of automatic current sharing, reduced RMS current and integrated magnetics.

Despite the advantages with three-phase LLC converter, it requires three individual inductors and three individual transformers, which increases system volume and cost a lot. Therefore, magnetic integration is necessary for application of three-phase LLC converter. But for present DC/DC converters operating at around 100 kHz, it is very difficult and expensive to achieve integrated magnetic with PCB windings since the magnetic is still bulky. Recent progress in high-frequency single-phase LLC converter with GaN devices and novel magnetic demonstrate significantly improved power density, while still maintaining a high efficiency [27]-[29]. Furthermore, other challenges in high-frequency LLC converter have also been addressed, including: digital control systems design [11], [30]-[34], PCB winding for MHz f_S [14], flux cancelation to reduce transformer size and losses [27]. Further efforts have been made to use a simple four-layer PCB winding to replace conventional 12-layer PCB winding, and integrate SRs and output capacitors into the secondary winding [28][29]. When using four-layer PCB windings, two shielding layers could be placed in between primary and secondary windings. Each shielding layer is connected to the primary ground. Therefore, the common-mode (CM) noise current can only circulate in the primary side [35]. The high-frequency transformer is further improved by integrating four transformers into one magnetic core [36], and a novel shielding technique is applied to reduce CM noise and improve efficiency [37].

By pushing f_S of three-phase LLC converter much higher than that of state-of-the-art, integrated magnetics with PCB winding and shielding technique can be applied to achieve high efficiency, high power density and reduced CM noise. In this paper, Section II investigates the three-phase interleaved LLC converter topologies and state-of-the-art magnetic integration. Section III employs a structure suitable for high-frequency operation, and proposes an integrated magnetic structure which can integrate three inductors and three transformers into one magnetic core with 4-layer PCB winding and additional 2-layer shielding. Section IV presents optimization method for the proposed magnetic structure. Section V presents experimental results on a 1MHz 400V/48V 3kW three-phase LLC converter prototype with a peak efficiency of 97.7% and a power density of 600W/inch^3. Both efficiency and power density of the proposed LLC converter have significant improvement compared to the state-of-the-art design practices. The summary is given in Section VI.

II. Investigation of Three-phase Interleaved LLC Converters and Magnetic Integration

There are many topologies of the three-phase interleaved LLC converter, these topologies provide a trade-off between the winding loss and core loss of the transformers to better optimize the magnetic components, which are the main challenge to achieve a high-efficiency high-power-density solution. First topology is proposed in [21] to interconnect the primary sides to a common floating Y-node, as shown in Fig. 2(a), and simply interleaving the primary switches will provide automatic current sharing between phases even there is tolerance in the resonant tanks of each phase. Additionally, it can help to reduce the RMS current, as shown in Fig. 2(b), by re-shaping the current waveform through the voltage fluctuation at Y-node to be more like rectangular waveforms [21][22], in which i_{Lr_1ph} is the resonant current of single-phase LLC converter with 1kW output power and i_{Lr_3ph} is that of three-phase LLC converter with 1kW output power per phase. It is shown that the peak current, as well as the RMS current of i_{Lr_3ph} are reduced compared to those of i_{Lr_1ph}, so that three-phase interleaved LLC converter will result in a smaller conduction loss.

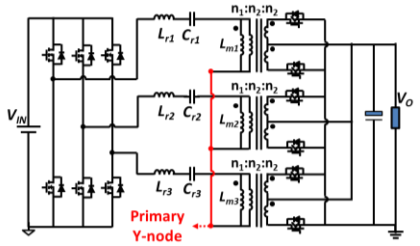

(a)

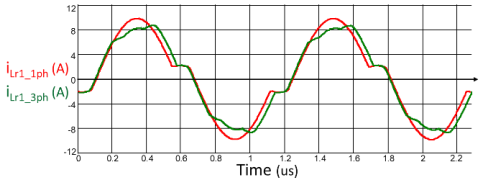

(b)

Fig. 2 Three-phase LLC converter with Y-Primary connection. (a) Topology. (b) Waveform.

Other topologies of three-phase LLC converter have been proposed by the industry [23][24]. By moving the Y-node to the secondary side as shown in Fig. 3(a) [23], it still has the benefit of automatic current sharing, however, the average voltage of secondary common Y-node is half of output voltage V_O, so that the effective secondary Y-node is same as that of voltage doubler structure in secondary side, which means the volt-

This article has been accepted for publication in a future issue of this journal, but has not been fully edited. Content may change prior to final publication. Citation information: DOI 10.1109/JESTPE.2019.2891317, IEEE Journal of Emerging and Selected Topics in Power Electronics

second applied to the transformer is reduced by half, and the transformer secondary winding current is doubled, leading to an increase in the winding losses. The operation of Δ-Cr network is equivalent to Y-Primary or Y-Secondary, however, the required capacitance of each resonant capacitor *Cr* in Δ-Cr network is just one third of that in Y-Primary. And since both terminals of each resonant capacitor are connected to the switching nodes, there is no DC bias in the resonant tank. Another topology is shown in Fig. 3(b) [24], in which the primary and secondary winding are connected in delta-connection. The benefit of the delta-connection is that the current is reduced by a factor of $\sqrt{3}$ which means the winding loss is reduced to one third, however the voltage*second on the transformer is increased by a factor of $\sqrt{3}$.

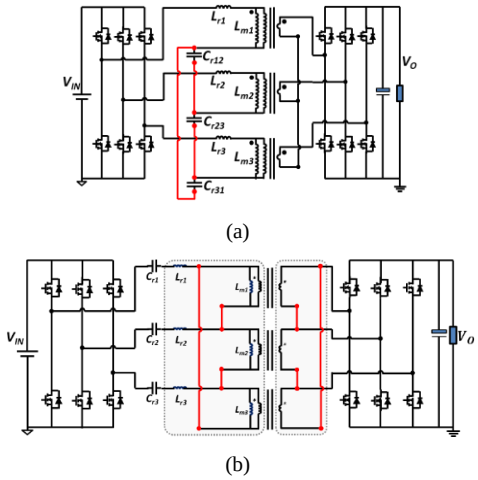

(a)

(b)

Fig. 3 Comparison of alternative three-phase LLC structures. (a) Δ-Cr network and Y-Secondary. (b) Δ-Primary and Δ-Secondary.

In summary, there are three options to interconnect the primary side: Y-Primary, primary Δ-Cr network, Δ-Primary; and two options to interconnect the primary side: Y-Secondary, Δ-Secondary. Using one of these five options can achieve automatic current sharing and re-shaped resonant current as shown in Fig. 2(b). Or any primary option and any secondary option can combine to also achieve automatic current sharing and re-shaped resonant current. The feature of different three-phase LLC converter structure is compared in TABLE I. The primary and secondary current in phase leg is I_{Pri} and I_{Sec}; transformer primary and secondary winding current is I_{Tx_Pri} and I_{Tx_Sec}; voltage applied to transformer primary and secondary winding at resonant frequency is V_{Tx_Pri} and V_{Tx_Sec}; input voltage is V_{IN} and output current is I_{OUT}.

TABLE I
Comparison of Different Three-phase Connection

Structure	Voltage	Current	Note
Y-Primary	$V_{Tx\_Pri} = V_{IN}/2$	$I_{Tx\_Pri} = I_{Pri}$	N/A
Δ-Cr network	$V_{Tx\_Pri} = V_{IN}/2$	$I_{Tx\_Pri} = I_{Pri}$	1/3 *Cr*, no DC bias
Δ-Primary	$V_{Tx\_Pri} = \sqrt{3}\cdot V_{IN}/2$	$I_{Tx\_Pri} = I_{Pri}/\sqrt{3}$	N/A
Y-Secondary	$V_{Tx\_Sec} = V_O/2$	$I_{Tx\_Sec} = I_{Sec}$	$I_{Sec} = 2\cdot I_{OUT}/3$
Δ-Secondary	$V_{Tx\_Sec} = \sqrt{3}\cdot V_O/2$	$I_{Tx\_Sec} = I_{Sec}/\sqrt{3}$	$I_{Sec} = 2\cdot I_{OUT}/3$

When employing three-phase interleaved LLC converter, the number of magnetic components increases by three times. In order to reduce the number of magnetic components, the three inductors and three transformers can be integrated into one three-phase inductor and one three-phase transformer, as shown in Fig. 4(a). Furthermore, an integrated magnetic structure is proposed in [23] to stack the three-phase inductor on top of the three-phase transformer so that all the magnetic components are integrated into one. Each of the three core legs in the middle represents either an inductor or a transformer, and the two outer legs are for magnetic shield. Such a structure, although can reduce the volume of magnetic components, is very complex to manufacture since it requires hand-wound transformer windings and bobbins, and additional assembling process to assemble the two pieces of magnetic components.

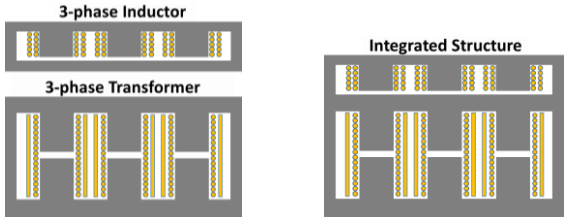

(a) (b)

Fig. 4 Integrated magnetic structure for three-phase LLC converter. (a) Before integration. (b) After integration.

Another way to reduce the number of magnetic components is to integrate one inductor and one transformer. Two U-I cores are combined into one E-I core in [38] as shown in Fig. 5(a), but for three-phase LLC converter, this would require three E-I cores. On the other hand, the air gaps for the center leg and outer leg need to be controlled separately, which increases the manufacturing complexity.

Adding leakage layer, also known as magnetic shunt, into transformer can also integrate inductor into transformer [39]-[44], as shown in Fig. 5(b). However, the vertical structure of transformer with leakage layer is very complex, all the components has to be stacked manually by hands. And along the vertical line, there are two air gaps that needs to be controlled separately. This labor intensive manufacturing process will increase the total cost, and reduce the reliability due to large tolerance during assembling.

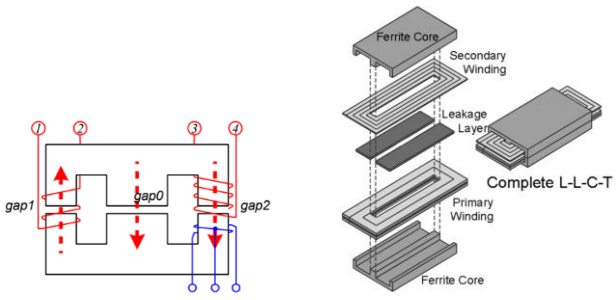

(a) (b)

Fig. 5 Magnetic structures to integrate inductor into transformer. (a) EI core structure [38]. (b) Transformer with leakage layer [40].

This article has been accepted for publication in a future issue of this journal, but has not been fully edited. Content may change prior to final publication. Citation information: DOI 10.1109/JESTPE.2019.2891317, IEEE Journal of Emerging and Selected Topics in Power Electronics

In conclusion, the three-phase interleaved LLC converters have superior performance over the single-phase LLC converter in terms of efficiency with the reduction of conduction losses with lower RMS current, and power density with the benefit of the flux cancellation to integrate magnetics. However, for state-of-the-art three-phase LLC converter operating below 100kHz, the magnetic component is still a challenge considering size and complexity. With the rapid development of wide-band-gap devices and its superior performance over the conventional Si-MOSFET, it's possible to push f_S up to MHz, therefore, the size of magnetic components can be reduced significantly, and the windings can be simply integrated into 4-layer PCB windings with additional 2-layer shielding. The following sections will present proposed magnetic integration for high-frequency three-phase LLC converter and its optimization process.

III. Proposed Magnetic Integration for High-frequency Three-phase LLC Converter

Base on the investigation in Section II, there are three options for secondary structures, half-bridge secondary, center-tap secondary and full-bridge secondary, as shown in Fig. 6 using EPC GaN devices. The AC current path at certain time interval is also plotted in Fig. 6. For half-bridge structure, the average voltage of secondary common Y-node is half of V_O, so that the effective secondary Y-node is same as that of voltage doubler structure in secondary side, and transformer voltage*second is reduced by half. But the SR current is doubled and the AC current path is longer, so it requires two EPC2029 GaN devices in parallel to handle the larger current. Larger AC current loop and paralleling SR devices are detrimental for high-frequency operation.

Compare to half-bridge structure, both center-tap and full-bridge secondary have much smaller AC current loop. While center-tap structure requires two sets of secondary windings per phase and double voltage rating of SR devices. Full-bridge structure requires only one set of secondary windings per phase and requires lower voltage rating SR devices, but at the cost of double number of SR devices. The SR voltage and current stresses, transformer turns ratio, voltage*second on transformer, SR device selection, number of devices and total SR conduction losses for these three structures are compared in TABLE II. Based on these analysis, full-bridge secondary is selected considering the trade-off between performance and cost.

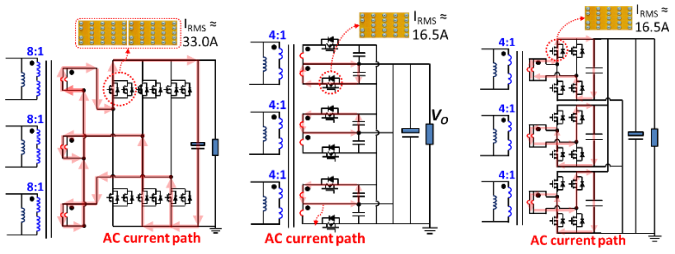

(a) (b) (c)

Fig. 6 Comparison of secondary structures. (a) Half-bridge secondary. (b) Center-tap secondary. (c) Full-bridge secondary.

TABLE II
Comparison of Secondary Structures

Secondary structure	Half-bridge	Center-tap	Full-bridge
SR voltage stress	V_O	$2 \cdot V_O$	V_O
SR current stress	33.0A	16.5A	16.5A
Transformer turns ratio	8:1	4:1	4:1
Voltage*second	$0.5 \cdot V_O / f_S$	V_O / f_S	V_O / f_S
SR device	EPC2029, 80V	EPC2034, 200V	EPC2029, 80V
SR device number	12	6	12
Total SR conduction loss	13.6W	22.9W	13.6W

Based on the aforementioned analysis, full-bridge secondary is selected due to efficiency consideration, Δ-Cr network is selected since it requires smaller resonant capacitance. The schematic is shown in Fig. 7, in which shielding is also added and highlighted by yellow color.

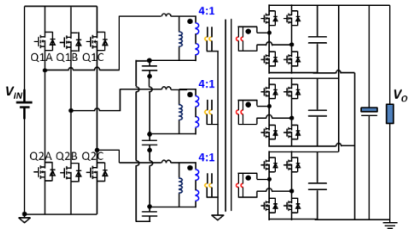

Fig. 7 Three-phase LLC converter with Δ-Cr network primary and full-bridge secondary.

When f_S is pushed much higher, there is opportunity to employ PCB windings to replace hand-wound windings and bobbins. Fig. 8 is an example of three-phase planar transformer. Each core leg is for the transformer of each phase, since the sum of flux for three phases is zero due to 120° phase shift, there is no need for additional core leg. The blue solid line represents primary windings and red dash line represents secondary windings.

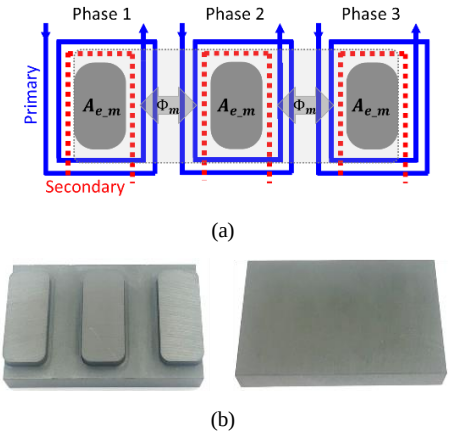

(a)

(b)

Fig. 8 Three-phase planar transformer. (a) Top view with simplified windings. (b) Magnetic cores.

For the design in Fig. 8, since the primary winding and secondary winding are perfectly interleaved, the leakage inductance is minimized. In order to regulate V_O for certain

This article has been accepted for publication in a future issue of this journal, but has not been fully edited. Content may change prior to final publication. Citation information: DOI 10.1109/JESTPE.2019.2891317, IEEE Journal of Emerging and Selected Topics in Power Electronics

range, the resonant inductor L_r must be properly designed [3], however, leakage inductance is normally not large enough to meet the requirement. Normally additional inductors are added in order to achieve regulation requirement. In this paper, a novel integrated magnetic structure is proposed for three-phase interleaved LLC converter as shown in Fig. 9. Compare to Fig. 8, the primary winding is extended, and an additional core leg is inserted for each phase. In the proposed structure, L_r can be controlled by the inductors effective cross-section areas A_{e_K} and air gaps l_{g_K}, and the magnetizing inductance L_m can be controlled by the transformer effective cross-section areas A_{e_m} and air gaps l_{g_m}. The ratio L_N between L_m and L_r is expressed in (1).

$$L_N = \frac{L_m}{L_r} = \frac{A_{e\_m}/l_{g\_m}}{A_{e\_r}/l_{g\_r}} \tag{1}$$

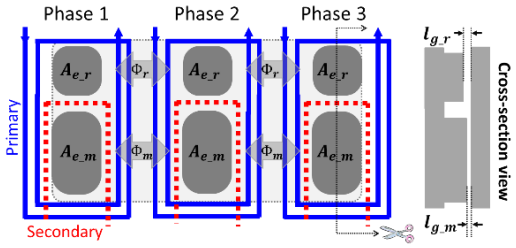

(a)

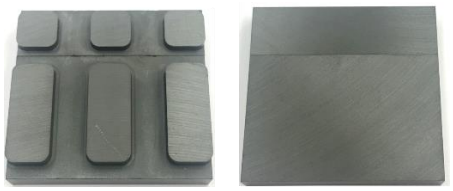

(b)

Fig. 9 Proposed three-phase integrated magnetic structure. (a) Top view with simplified windings and cross-section view. (b) Magnetic cores.

PCB windings has large overlap area between primary winding and secondary windings, thus large inter-winding capacitance. Since the primary side employs half-bridge structure, there is high *dv/dt* in the primary switching node for each phase. And these high *dv/dt* would induce large common-mode (CM) current, flowing from the three switching nodes in the primary side, through transformer inter-winding cap, to the secondary side, and coming back through LISN to the primary switching nodes, as shown in Fig. 10. For each phase, full-bridge secondary structure has complemental *dv/dt* at the two switching nodes, so these two *dv/dt* nodes cancel each other and there is no CM noise generated from the secondary side.

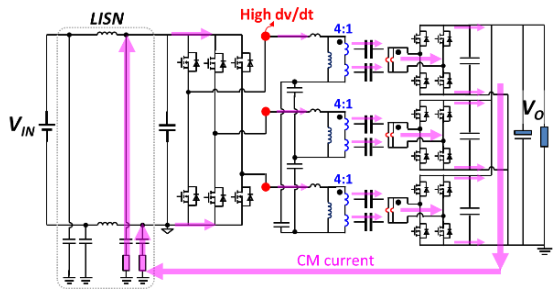

(a)

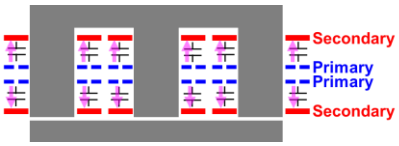

(b)

Fig. 10 CM current in three-phase LLC converter with PCB winding transformer. (a) Conduction path in schematics. (b) Cross-section view of transformer.

The shielding technique is an effective method to suppress CM noise. It is achieved by inserting shielding layers in between the primary and the secondary windings [35][37] as shown in Fig. 11. Since in this case the noise sources are in the primary side, all shielding layers are connected to the primary ground. Therefore, the CM noise current induced by the primary winding will flow to the shielding layer and then circulate back to the primary ground. The shielding layers are made identical to the secondary windings, so they have the same voltage potential distribution along the windings. Therefore, even there is a parasitic capacitance between the shielding layers and the secondary windings, there is no CM current between them since the voltage potential difference across this parasitic capacitance is zero.

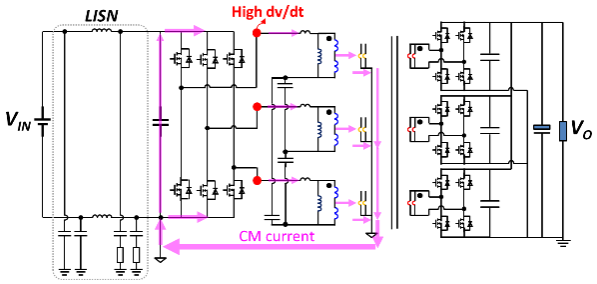

(a)

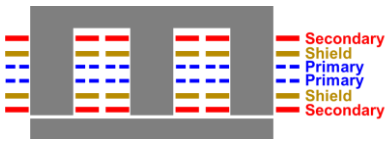

(b)

Fig. 11 Shielding eliminates CM current in three-phase LLC converter with PCB winding transformer and shielding. (a) Conduction path in schematics. (b) Cross-section view of transformer with shielding.

Fig. 12 shows the voltage distribution on secondary winding and shielding for one phase of the proposed transformer, and

This article has been accepted for publication in a future issue of this journal, but has not been fully edited. Content may change prior to final publication. Citation information: DOI 10.1109/JESTPE.2019.2891317, IEEE Journal of Emerging and Selected Topics in Power Electronics

the primary winding is not included for simplicity. Two terminals of secondary windings are marked as *A* and *B*, and those of shielding are marked as *A'* and *B'*. The center parts of two shielding layers are connected to primary ground. The windings can be stretched along the *x*-axis to map the voltage potential at each point on the windings to the *U*-*x* coordinate at the right side of Fig. 12. Since the secondary winding and shielding are identical, the voltage potentials of both at the same position on the *x*-axis are identical, so the two curves on the *U*-*x* coordinate overlap each other, and have $U = V$ at $x = 0$ and $U = -V$ at $x = L$.

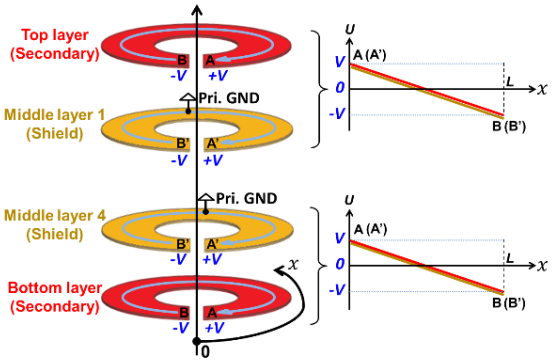

Fig. 12 Voltage potential on secondary windings and shielding.

Based on the proposed magnetic and shielding structure, the PCB winding and shielding implementation is shown in Fig. 13. The windings for one phase is shown here for simplicity, and those for the other two phases are same as Fig. 13. Comparing to the state-of-the-art designs, the proposed magnetic structure only requires 6-layer PCB winding, which is cheaper and does not require assembling; the customized core can be either molded as one set of core or assembled with two traditional E-I cores. In mass productions, since the cost of magnetic core is mainly determined by volume, the proposed magnetic structure is cheaper than the state-of-the-art designs due to smaller volume at much higher f_S. The manufacturing process is also much simpler compared to hand-wound transformers or transformers with magnetic shunt.

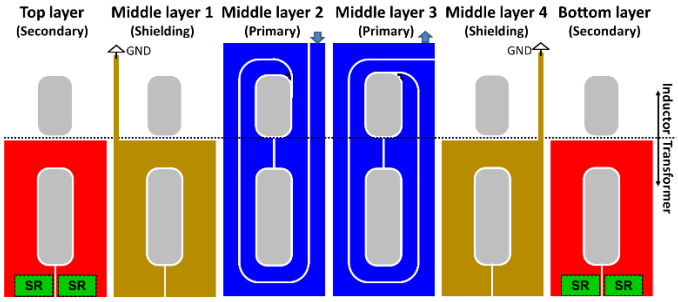

Fig. 13 PCB winding and shielding implementation for one phase of the proposed integrated magnetic structure.

IV. Optimization of Proposed Magnetic Structure for Three-phase LLC Converter

This section provides an optimization process for the integrated one core structure. Fig. 14 shows a survey of the suitable magnetic materials for this application [45]. ML91 is selected due to its core loss. The core loss P_{Core} can be calculated based on core loss density P_V and core volume V_{Core} using:

$$P_{Core} = P_V \cdot V_{Core} \tag{2}$$

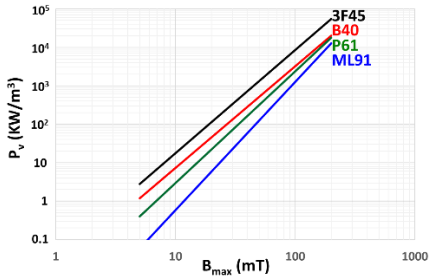

Fig. 14 Core loss measurement under 1MHz excitation.

The transformer losses are calculated with methods in [36][46]. In the application of high-power and low-voltage, the winding loss is dominant over the core loss, therefore, the transformer cross section area should be chosen in order to ensure that the maximum flux density inside the core does not go beyond the maximum allowable limit for the core material. Fig. 15 shows the optimization of the transformer total loss under full load condition based on its dimensions. Since the transformer has three dimension variables, core leg length *a*, winding width *c* and effective area *Ae*, *Ae* is first fixed to 250mm^2 to derive Fig. 15 and swept later to cover all the scenarios.

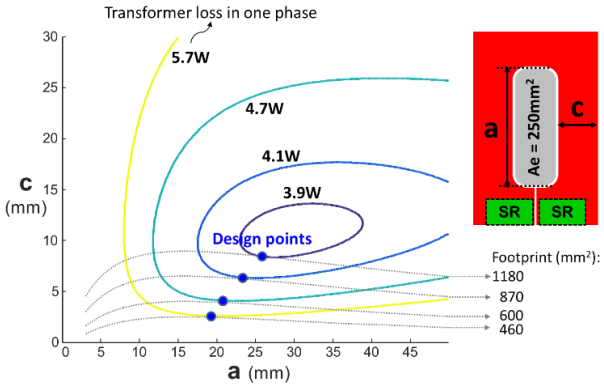

Fig. 15 Transformer optimization with given Ae of 250mm^2.

Then from the tangential point we can draw the minimum loss contour for each footprint for a fixed cross section area. Furthermore, different *Ae* (corresponding to different P_V value) are swept to get the optimal P_V for different footprint as shown in Fig. 16. For smaller footprint, the optimal *Ae* is smaller and corresponding P_V is larger. The shaded area will be selected as the design region for this paper.

This article has been accepted for publication in a future issue of this journal, but has not been fully edited. Content may change prior to final publication. Citation information: DOI 10.1109/JESTPE.2019.2891317, IEEE Journal of Emerging and Selected Topics in Power Electronics

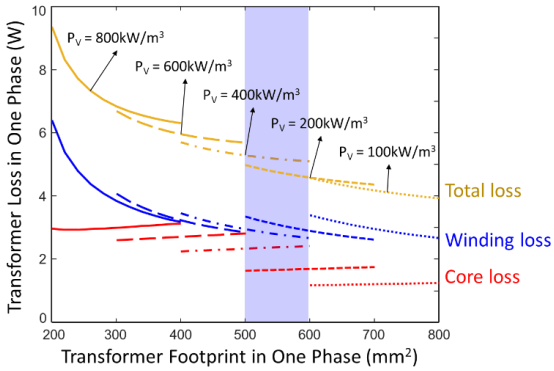

Fig. 16 Transformer minimum loss vs. footprint under different P_V.

The input of three-phase LLC converter, is normally regulated by the front-end power factor correction (PFC) to be 400V; therefore, the three-phase LLC converter needs to regulate V_O over a wide range, normally, from 40 V to 60 V, which corresponding to an input-to-output gain range of 0.8 to 1.2 as shown in Fig. 17(a). The 48V batteries normally have a nominal voltage of around 53.5V; in order to make three-phase LLC converter have a reduced gain range and operate at unit gain point for nominal V_O, the input of three-phase LLC converter can be regulated to have a range of 400V to 440V by controlling the output of PFC, as shown in Fig. 17(b). By doing that 600 V or 650 V devices can still be used for the PFC stage and the primary side of the DC-DC stage.

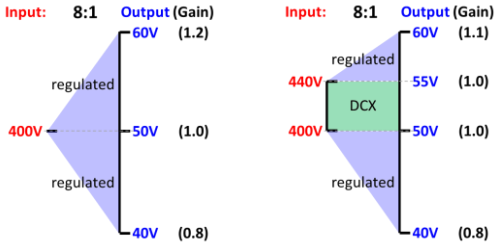

(a) (b)

Fig. 17 Output-to-input gain of three-phase LLC converter. (a) Fixed V_{IN} of 400V. (b) Variable V_{IN} of 400V to 440V.

Base on gain range requirement, the parameters of LLC converter can be designed following the methodology in [3]. The L_m is selected to be 25uH and L_r is selected to be 2.5uH. Wide f_S range at light load condition can be solved with burst mode [34]. Since the transformer width b and winding width c are determined from transformer optimization, those two variables are already determined for inductor part. Then the inductor can be optimized with different core leg length a_i. 2D finite element analysis (FEA) is employed to get the inductor winding loss for given winding width c. And core loss is derived based on equation (2). The total footprint is calculated based on total width b, winding width c, and core leg length a_i. Then the inductor loss vs. footprint can be plotted as shown in Fig. 18.

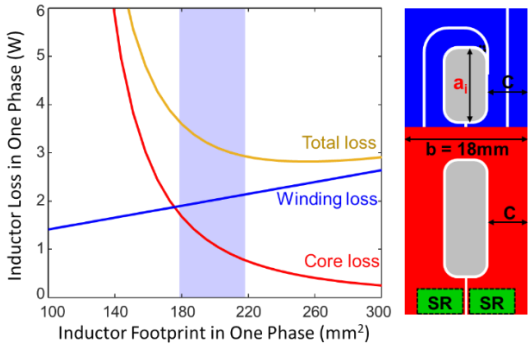

Fig. 18 Inductor Loss vs. footprint.

The flowchart for the optimization process of proposed magnetic structure is shown in Fig. 19. Based on the proposed integrated magnetic structure and design methodology, a 3kW three-phase interleaved LLC converter is designed, and the specifications are shown in TABLE III. The primary side uses 600V GaN devices PGA26E07BA from Panasonic, and the secondary side uses 80V GaN devices EPC2029 from EPC.

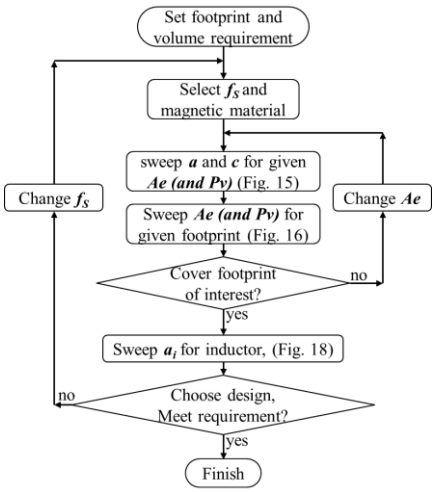

Fig. 19 Flowchart for whole optimization process.

TABLE III
Specifications of the Proposed Three-phase LLC Converter

Component	Parameters
Resonant Frequency	1MHz
Dead Time	60ns
Transformer turns ratio	4:1
Primary devices	PGA26E07BA
Secondary devices	EPC2029
Primary Driver	Si8273GBD
Secondary Drivers	LM5113
Resonant Capacitor	3nF
Resonant Inductance	2.5uH
Magnetizing Inductance	25uH

To verify the design, 3D FEA simulation is employed to show the current distribution in windings. The current distribution on top surface and bottom surface of each winding layer is shown in Fig. 20, and the total winding loss of each layer is shown in TABLE IV. It is worth noting that the air gap of both transformer part and inductor part is close to Layer 6, so

This article has been accepted for publication in a future issue of this journal, but has not been fully edited. Content may change prior to final publication. Citation information: DOI 10.1109/JESTPE.2019.2891317, IEEE Journal of Emerging and Selected Topics in Power Electronics

Layer 6 has larger winding loss compared to Layer 1, and Layer 4 has larger winding loss compared to Layer 3.

TABLE IV
Winding and Termination Losses

Component	Loss
Winding Layer 1 (Secondary)	1.3W
Winding Layer 2 (Shielding)	0.2W
Winding Layer 3 (Primary + inductor)	1.8W
Winding Layer 4 (Primary + inductor)	2.8W
Winding Layer 5 (Shielding)	0.2W
Winding Layer 6 (Secondary)	1.5W
Primary Termination	0.3W
Secondary Termination	1.1W

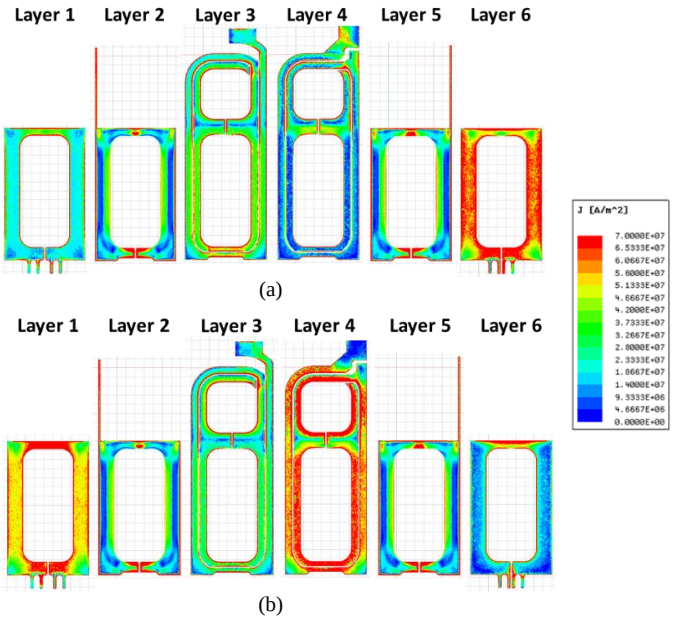

(a)

(b)

Fig. 20 3D FEA simulation of current distribution on surfaces of different winding layers. (a) Top surface. (b) Bottom surface.

V. Experimental Results

3kW 400V/48V LLC converter prototype operating at 1MHz is shown in Fig. 21, which has achieved a power density of 600W/inch^3 (37kW/L). It has a length of around 71mm, a width of around 55mm, and a height of less than 17.7mm.

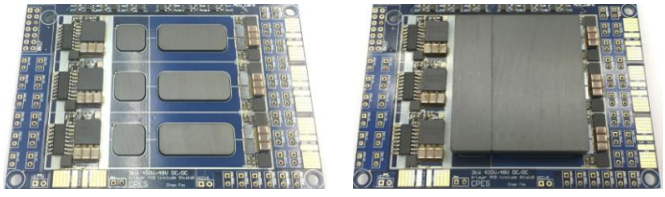

(a) (b)

Fig. 21 1MHz 3kW 400V/48V LLC converter prototype. (a) Prototype Without top magnetic plate. (b) Fully-assembled prototype.

The experimental waveforms of drain-source voltage for primary low-side switch of phase B V_{ds_Q2B}, drain-source voltage for one SR of phase B V_{ds_SR2B}, resonant current for three phases i_{Lr_A}, i_{Lr_B}, i_{Lr_C}, under full-load and light-load (20% load) conditions are shown in Fig. 22. Here, it shows the inherent benefit of LLC converter that it can achieve ZVS for both primary and secondary switches all load conditions. The resonant current of three phases have almost identical shape. The efficiency of the proposed three-phase interleaved LLC converter is shown in Fig. 23. The proposed LLC converter has a peak efficiency of 97.7%, a full-load efficiency of 97.2% and a light-load (10% load) efficiency of 93.0%.

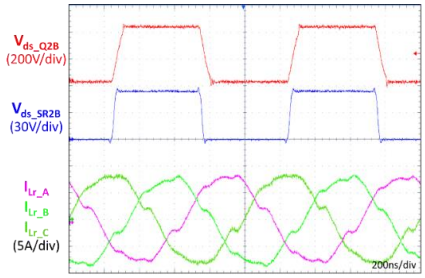

(a)

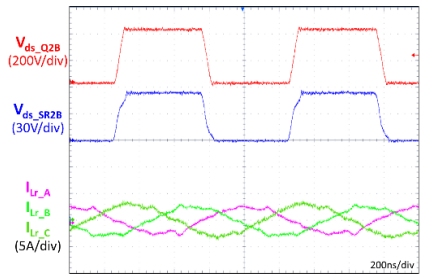

(b)

Fig. 22 Experimental waveforms at resonant frequency. (a) Full-load. (b) Light-load (20% load).

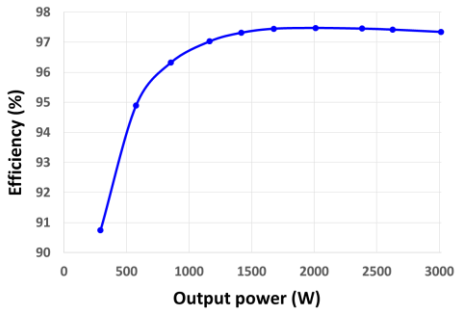

Fig. 23 Measured efficiency for 53.5V output at f_O.

The experimental waveforms of f_S = 0.8MHz and f_S = 1.6MHz under full-load condition are shown in Fig. 24. It shows that ZVS for both primary and secondary switches can be achieved and the resonant current between three phases are well balanced under different operating conditions. The efficiency and f_S for the whole V_O range under full-load condition are shown in Fig. 25.

This article has been accepted for publication in a future issue of this journal, but has not been fully edited. Content may change prior to final publication. Citation information: DOI 10.1109/JESTPE.2019.2891317, IEEE Journal of Emerging and Selected Topics in Power Electronics

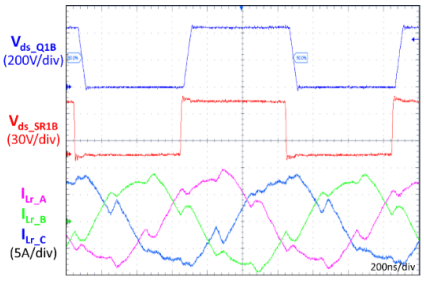

(a)

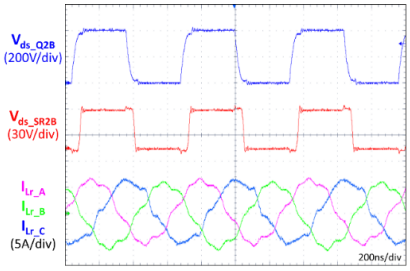

(b)

Fig. 24 Experimental waveforms of f_S = 0.8MHz and f_S = 1.6MHz under full-load condition. (a) f_S = 0.8MHz. (b) f_S = 1.6MHz.

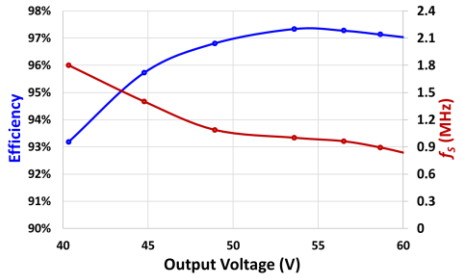

Fig. 25 Measured full-load efficiency and f_S at different Vo.

VI. Conclusion

The LLC converter is very popular as DC/DC converter in server and telecom applications due to its high efficiency and high power density. It has been demonstrated in literature that three-phase interleaved LLC converter has the potential to increase efficiency. Besides this, it can reduce input and output current ripples and achieve automatic current sharing. But changing from single-phase to three-phase LLC converter requires three times magnetic components. This paper proposes a planar magnetic structure that can integrate three inductors and three transformers into one magnetic core by utilizing the properties of GaN devices with a much higher f_S. Furthermore, all the magnetics can be implemented with 4-layer PCB winding, and additional 2-layer shielding can be integrated to reduce CM noise. Detailed design optimization and FEA analysis are also provided.

The proposed three-phase interleaved LLC converter with integrated magnetics can demonstrate the impact of GaN devices in several important issues such as efficiency, power density and manufacturability. With the academic contribution of this paper, we can design 400V/48V DC/DC converter of more than 10 times higher in f_S and power density, while at the same time maintaining a higher efficiency, compared to the state-of-the-art design practices using silicon devices. A 1MHz 3kW 400V/48V three-phase LLC converter with the proposed magnetic structure is designed, and a peak efficiency of 97.7% and a power density of 600W/inch^3 are achieved.

References

[1] B. Yang, F. C. Lee, A. J. Zhang, and G. Huang. "LLC resonant converter for front end DC/DC conversion." in *Proc. IEEE APEC, 2002*, pp. 1108-1112.

[2] B. Yang, Y. Ren, and F. C. Lee, "Integrated magnetic for LLC resonant converter," in *Proc. IEEE APEC, 2002*, pp. 346–351.

[3] B. Lu, W. Liu, Y. Liang, F. C. Lee, and J. D. Van Wyk. "Optimal design methodology for LLC resonant converter." In *Proc. IEEE APEC, 2006*, pp. 533-538.

[4] D. Fu, B. Lu, and F. C. Lee. "1MHz high efficiency LLC resonant converters with synchronous rectifier." In *Proc. IEEE PESC, 2007*, pp. 2404-2410.

[5] F. C. Lee, S. Wang, P. Kong, C. Wang, and D. Fu, "Power architecture design with improved system efficiency, EMI and power density," in *Proc. IEEE PESC, 2008*, pp. 4131–4137.

[6] Chao Fei, "Optimization of LLC Resonant Converters: State-trajectory Control and PCB based Magnetics." Dissertation, Virginia Tech, 2018.

[7] Ernest Orlando Lawrence Berkeley National Laboratory. "United States Data Center Energy Usage Report," June 2016.

[8] Vicor white paper, "From 48V direct to Intel VR12.0: Saving 'Big Data' $500000 per data center, per year," July 2012, [online]: http://www.vicorpower.com/documents/whitepapers/wp_VR12.pdf

[9] D. Kim, J. He, and D. G. Figueroa, "48V Power Delivery to Grantley Reference Board," 2016.

[10] X. Li and S. Jiang, "Google 48V Power Architecture", In *Proc. IEEE APEC, 2017*, plenary session, [online]: https://www.apec-conf.org/Portals/0/APEC%202017%20Files/Plenary/APEC%20Plenary%20Google.pdf?ver=2017-04-24-091315-930&timestamp=1495563027516

[11] C. Fei, M. H. Ahmed, F. C. Lee, and Q. Li, "Two-stage 48V-12V/6V-1.8V Voltage Regulator Module with Dynamic Bus Voltage Control for Light Load Efficiency Improvement of Two-stage Voltage Regulator," *IEEE Trans. Power Electron.*, vol. 32, no. 7, pp. 5628-5636, Jul. 2017.

[12] M. H. Ahmed, C. Fei, F. C. Lee, and Q. Li, "48-V Voltage Regulator Module With PCB Winding Matrix Transformer for Future Data Centers," *IEEE Trans. Ind. Electron.*, vol. 64, no. 12, pp. 9302-9310, Dec. 2017.

[13] S. Saggini, O. Zambetti, R. Rizzolatti, M. Picca, and P. Mattavelli, "An Isolated Quasi-Resonant Multi-Phase Single-Stage Topology for 48 V VRM Applications," *IEEE Trans. Power Electron.*, vol. 33, no. 7, pp. 6224-6237, Jul. 2018.

[14] F. C. Lee, Q. Li, Z. Liu, Y. Yang, C. Fei and M. Mu, "Application of GaN devices for 1 kW server power supply with integrated magnetics," *CPSS Transactions on Power Electronics and Applications*, vol. 1, no. 1, pp. 3-12, Dec. 2016.

[15] J. Biela, U. Badstuebne, and J. W. Kolar, "Design of a 5-kW, 1-U, 10-kW/dm^3 Resonant DC–DC Converter for Telecom Applications," *IEEE Trans. on Power Electron.*, vol. 24, no. 7, pp. 1701-1710, Jul. 2009.

[16] K. H. Yi, and G. W. Moon. "Novel two-phase interleaved LLC series-resonant converter using a phase of the resonant capacitor." *IEEE Trans. Ind. Electron.*, vol. 56, no. 5, pp. 1815-1819, May 2009.

[17] Z. Hu, Y. Qiu, L. Wang, and Y. F. Liu, "An Interleaved LLC Resonant Converter Operating at Constant Switching Frequency," *IEEE Trans. Power Electron.*, vol. 29, no. 6, pp. 2931-2943, Jul. 2014.

[18] Z. Hu, Y. Qiu, Y. F. Liu, and P. C. Sen, "A control strategy and design method for interleaved LLC converters operating at variable switching frequency," *IEEE Trans. Power Electron.*, vol. 29, no. 8, pp. 4426-4437, Aug. 2014.

[19] H. Wu, X. Zhan, and Y. Xing, "Interleaved LLC Resonant Converter With Hybrid Rectifier and Variable-Frequency Plus Phase-Shift Control

for Wide Output Voltage Range Applications," *IEEE Trans. Power Electron.*, vol. 32, no. 6, pp. 4246-4257, Jun. 2017.
[20] O. Kirshenboim, and M. M. Peretz, "Combined Multi-Level and Two-phase Interleaved LLC Converter with Enhanced Power Processing Characteristics and Natural Current Sharing," *IEEE Trans. Power Electron.*, vol. 33, no. 7, pp. 5613-5620, Jul. 2018.
[21] E. Orietti, P. Mattavelli, G. Spiazzi, C. Adragna, and G. Gattavari, "Current sharing in three-phase LLC interleaved resonant converter," in *Proc. IEEE ECCE*, 2009, pp 1145-1152.
[22] H. S. Kim, J. W. Baek, M. H. Ryu, J. H. Kim, and J. H. Jung, "The high-efficiency isolated ac–dc converter using the three-phase interleaved LLC resonant converter employing the Y-connected rectifier," *IEEE Trans. Power Electron.*, vol. 29, no. 8, pp. 4017-4028, Aug. 2014.
[23] H. Yang, C. Pei, and Y. Liang, "Magnetic integrated device and power conversion circuit," U.S. Patent Application No. 15/147,589.
[24] K. Boysen, R. Myhre, "Resonant circuit and resonant DC/DC converter." US patent application, US 2016/9240723 B2.
[25] Y. Nakakohara, H. Otake, T. M. Evans, T. Yoshida, M. Tsuruya, and K. Nakahara, "Three-phase LLC series resonant DC/DC converter using SiC MOSFETs to realize high-voltage and high-frequency operation," *IEEE Trans. Ind. Electron.*, vol. 63, no. 4, pp. 2103-2110, Apr. 2016.
[26] M. Noah, S. Endo, H. Ishibashi, K. Nanamori, J. Imaoka, K. Umetani and M. Yamamoto, "A Current Sharing Method Utilizing Single Balancing Transformer for a Multiphase LLC Resonant Converter with Integrated Magnetics," *IEEE Journal of Emerging and Selected Topics in Power Electronics*, to be published.
[27] D. Reusch and F. C Lee, "High frequency bus converter with low loss integrated matrix transformer," in *Proc. IEEE APEC 2012*, pp. 1392–1397.
[28] D. Huang, S. Ji, and F. C. Lee. "LLC resonant converter with matrix transformer," *IEEE Trans. on Power Electron.*, vol. 29, no. 8, pp. 4339-4347, Aug. 2014.
[29] M. Mu and F. C. Lee. "Design and Optimization of a 380V-12V High-Frequency, High-Current LLC Converter with GaN Devices and Planar Matrix Transformers," *IEEE Journal of Emerging and Selected Topics in Power Electronics*, vol. 4, no. 3, pp. 854-862, Sep. 2016.
[30] H. De Groot, E. Janssen, R. Pagano, and K. Schetters. "Design of a 1-MHz LLC resonant converter based on a DSP-driven SOI half-bridge power MOS module," *IEEE Trans. on Power Electron.*, vol. 22, no. 6, pp. 2307-2320, Nov. 2007.
[31] C. Fei, F. C. Lee, and Q. Li. "Digital Implementation of Soft Start-up and Short-circuit Protection for High-frequency LLC Converters with Optimal Trajectory Control (OTC)." *IEEE Trans. on Power Electron.*, vol. 32, no. 10, pp. 8008-8017, Oct. 2017.
[32] C. Fei, F. C. Lee, and Q. Li. "Multi-step Simplified Optimal Trajectory Control (SOTC) for fast transient response of high frequency LLC converters." In *Proc. IEEE ECCE 2015*, pp. 2064-2071.
[33] C. Fei, Q. Li and F. C. Lee. " Digital Implementation of Adaptive Synchronous Rectifier (SR) Driving Scheme for High-frequency LLC Converters with Microcontroller," *IEEE Trans. on Ind. Electron.*, vol. PP, no. 99, pp. 1–1, 2017.
[34] C. Fei, F. C. Lee, and Q. Li. " Digital Implementation of Light-Load Efficiency Improvement for High-Frequency LLC Converters with Simplified Optimal Trajectory Control." *IEEE Journal of Emerging and Selected Topics in Power Electronics*, accepted.
[35] Y. Yang, D. Huang, F. C. Lee, Q. Li, "Analysis and reduction of common mode EMI noise for resonant converters," in *Proc. IEEE APEC, 2014*, pp.566-571.
[36] C. Fei, F. C. Lee and Q. Li. "High-efficiency High-power-density LLC Converter with an Integrated Planar Matrix Transformer for High Output Current Applications," *IEEE Trans. on Ind. Electron.*, vol. 64, no. 11, pp. 9072-9082, Nov. 2017.
[37] C. Fei, Y. Yang, F. C. Lee and Q. Li. "Shielding Technique for Planar Matrix Transformers to Suppress Common-Mode EMI Noise and Improve Efficiency," *IEEE Trans. on Ind. Electron.*, vol. 65, no. 2, pp. 1263-1272, Feb. 2018.
[38] B. Yang, R. Chen, and F. C. Lee. "Integrated magentics for LLC resonant converter." In *Proc. IEEE APEC 2002*, pp. 346-351.
[39] J. T. Strydom, and J. D. Van Wyk. "Electromagnetic design optimization of planar integrated power passive modules." In *Proc. IEEE PESC 2002*, pp. 573-578.
[40] R. Chen, J. T. Strydom, and J. D. Van Wyk. "Design of planar integrated passive module for zero-voltage-switched asymmetrical half-bridge PWM converter." *IEEE trans. on Ind. App.*, vol. 39, no. 6, pp. 1648-1655, Nov. / Dec. 2003.
[41] W. Liu, J. D. Van Wyk, and W. G. Odendaal. "Design and evaluation of integrated electromagnetic power passives with vertical surface interconnections." In *Proc. IEEE APEC 2004*, pp. 958-963.
[42] D. Huang, P. Kong, F. C. Lee, and D. Fu. "A novel integrated multi-elements resonant converter." In *Proc. IEEE ECCE 2011*, pp. 3808-3815.
[43] D. Huang, D. Gilham, W. Feng, P. Kong, D. Fu, and F. C. Lee. "High power density high efficiency dc/dc converter." *Proc. IEEE ECCE 2011*, pp. 1392-1399.
[44] M. Li, Z. Ouyang, M. A. E. Andersen. "High frequency LLC resonant converter with magnetic shunt integrated planar transformer." *IEEE Trans. on Power Electron.*, early access.
[45] M. Mu, Q. Li, D. J. Gilham, F. C. Lee, and K. D. Ngo, "New core loss measurement method for high-frequency magnetic materials," *IEEE Trans. on Power Electron.*, vol. 29, no. 8, pp. 4374-4381, Aug. 2014.
[46] P. L. Dowell, "Effects of eddy currents in transformer windings," *Electrical Engineers, Proceedings of the Institution of*, vol.113, no.8, pp.1387-1394, Aug. 1966.

Chao Fei (S'13-M'18) received the B.S. degree in electrical engineering from Zhejiang University, Hangzhou, China, in 2012, and the M.S. degree and Ph.D. degree in electrical engineering from Center for Power Electronics Systems (CPES), Virginia Tech, Blacksburg, VA, USA, in 2015 and 2018, respectively.

He is now a Hardware Engineer at Google Inc., Mountain View, CA, USA. His research interests include high-frequency power conversion, resonant converters, digital control, power management and wireless charging.

Rimon Gadelrab (S'14) was born in Alexandria, Egypt, in 1990. He received the B.S. and M.S. degrees in electrical engineering from Alexandria University, Alexandria, Egypt, in 2012 and 2015, respectively. He is currently working toward the Ph.D. degree in the Center for Power Electronics Systems, Virginia Tech. His main research interests include high frequency, high-power density high-efficiency power conversion.

Qiang Li (M'11) received the B.S. and M.S. degrees in power electronics from Zhejiang University, Hangzhou, China, in 2003 and 2006, respectively, and the Ph.D. degree in electrical engineering from Virginia Tech, Blacksburg, VA, USA, in 2011.

He is currently an Associate Professor in the Center for Power Electronics Systems, Virginia Tech, Blacksburg, VA, USA. His research interests include high-density electronics packaging and integration, high-frequency magnetic components, and high-frequency power conversion.

Fred C. Lee (S'72–M'74–SM'87–F'90–LF'12) received the B.S. degree in electrical engineering from the National Cheng Kung University, Tainan, Taiwan, in 1968, and the M.S. and Ph.D. degrees in electrical engineering from Duke University, Durham, NC, USA, in 1972 and 1974, respectively.

He is currently a University Distinguished Professor at Virginia Tech, Blacksburg, USA, and the Director of the Center for Power

Electronics Systems (CPES), a National Science Foundation Engineering Research Center (NSF ERC) established in 1998, with four university partners—University of Wisconsin-Madison, Rensselaer Polytechnic Institute, North Carolina A&T State University, University of Puerto Rico-Mayagüez—and more than 80 industry members. The Center's vision is "to provide leadership through global collaboration to create electric power processing systems of the highest value to society." Over the ten-year NSF ERC Program, CPES has been cited as a model ERC for its industrial collaboration and technology transfer, as well as education and outreach programs. His research interests include high-frequency power conversion, distributed power systems, renewable energy, power quality, high-density electronics packaging and integration, and modeling and control. He holds 82 U.S. patents and has published 296 journal articles and more than 722 refereed technical papers. During his tenure at Virginia Tech, he has supervised to completion 84 Ph.D. and 93 Master's students.

Dr. Lee received the William E. Newell Power Electronics Award in 1989, the Arthur E. Fury Award for Leadership and Innovation in Advancing Power Electronic Systems Technology in 1998, and the Ernst-Blickle Award for achievement in the field of power electronics in 2005. He has served as the President of the IEEE Power Electronics Society (1993–1994). He was named to the U.S. National Academy of Engineering in 2011. He was named to the Academia Sinica of Taiwan in 2012. He was also named to Chinese Academy of Engineering in 2013.